EUROPEAN ORGANIZATION FOR NUCLEAR RESEARCH
Laboratory for Particle Physics

Departmental Report

CERN/AT 2007-18 (MCS)

IN-SITU NEUTRON DIFFRACTION UNDER TENSILE LOADING OF POWDER-IN-TUBE Cu/Nb_3Sn COMPOSITE WIRES: EFFECT OF REACTION HEAT TREATMENT ON TEXTURE, INTERNAL STRESS STATE AND LOAD TRANSFER

C. Scheuerlein[1], U. Stuhr[2], L. Thilly[3]

The strain induced degradation of Nb_3Sn superconductors can hamper the performance of high field magnets. We report elastic strain measurements in the different phases of entire non-heat treated and fully reacted Nb_3Sn composite strands as a function of uniaxial stress during in-situ deformation under neutron beam. After the reaction heat treatment the Cu matrix loses entirely its load carrying capability and the applied stress is transferred to the remaining Nb-Ta alloy and to the brittle $(Nb\text{-}Ta)_3Sn$ phase, which exhibits a preferential <110> grain orientation parallel to the strand axis.

1 CERN, Accelerator Technology Departement, Geneva, Switzerland
2 Laboratory of Neutron Scattering, ETH Zürich & Paul Scherrer Institute, Villigen PSI, Switzerland
3 Laboratoire de Métallurgie Physique, Université de Poitiers, Futuroscope, France

Accepted for publication in Applied Physics Letters

CERN, Accelerator Technology Department
CH - 1211 Geneva 23
Switzerland

26 July 2007

The strain induced degradation of the critical properties of Nb_3Sn superconducting cables can be a severe limitation for their application in high field magnets for particle accelerators or fusion devices. Critical current density (J_c) measurements of the brittle Nb_3Sn composite strands are also strongly influenced by external stress.[1] Since the 3-D stress state in the strand sample mounted on measurement mandrels is often not well known, the Nb_3Sn strain sensitivity causes a major uncertainty in J_c measurements.

Large strain gives rise to an irreversible J_c degradation caused by cracks in the brittle Nb_3Sn. The reversible Nb_3Sn degradation at lower strains has been attributed to elastic distortions of the A15 Nb_3Sn lattice.[2, 3] It appears that the strain dependence of Nb_3Sn multifilament strands is influenced by the processing route. Nb_3Sn strands of the "bronze route" design are for instance assumed to be less affected by strain than Nb_3Sn strands of the "internal Sn" design, but the reasons for the different behaviour are not well understood. In order to reduce the Nb_3Sn strain sensitivity it is important to understand the degradation mechanisms and the influence of the strand design on the superconductor degradation under mechanical loading.

High resolution neutron diffraction can be used for accurate measurements of the 3-dimensional stress state in composite materials and the elastic strain in the different phases of Nb_3Sn composite strands has been studied.[4, 5] However, because of the limited neutron flux, such measurements usually require a relatively large sample volume, a problem that has been bypassed by the use of bundles of typically 100 strand samples. With such a configuration it is however not possible to apply a well defined tensile load to the strands. Recently, with the time-of-flight diffractometer with multiple pulse overlap (POLDI)[6, 7] at the Swiss spallation neutron source SINQ of the Paul Scherrer Institut (PSI) it became possible to perform high resolution diffraction experiments with a single composite wire in axial and transverse directions during in-situ tensile loading.[8]

In the present article we report the evolution of elastic strain upon tensile loading in axial and transverse directions in the different crystallographic phases of a state-of-the-art Nb_3Sn strand of the powder-in-tube (PIT) design [9] before and after reaction heat treatment.

The non heat treated strand has been manufactured by Shape Metal Innovation (SMI), B. V., the Netherlands (now European Advanced Superconductors (EAS), Germany). The strand has a nominal diameter of 1 mm and the Cu to non-Cu volume ratio is 0.73. It consists of a Cu matrix with 192 embedded Nb-7.5wt.%Ta tubes. The tubes are filled with a mixture of $NbSn_2$ and Sn particles. During a 675 °C reaction heat treatment (HT) lasting 84 h, about 67 vol.% of the tubes are transformed into the brittle intermetallic phase $(Nb\text{-}Ta)_3Sn$, while 33 vol.% remain un-reacted ductile Nb-Ta alloy (see Figure 1). During the fabrication processes and the subsequent strand heat treatment the Nb-Ta filaments and the Cu matrix are strongly bonded with each other.

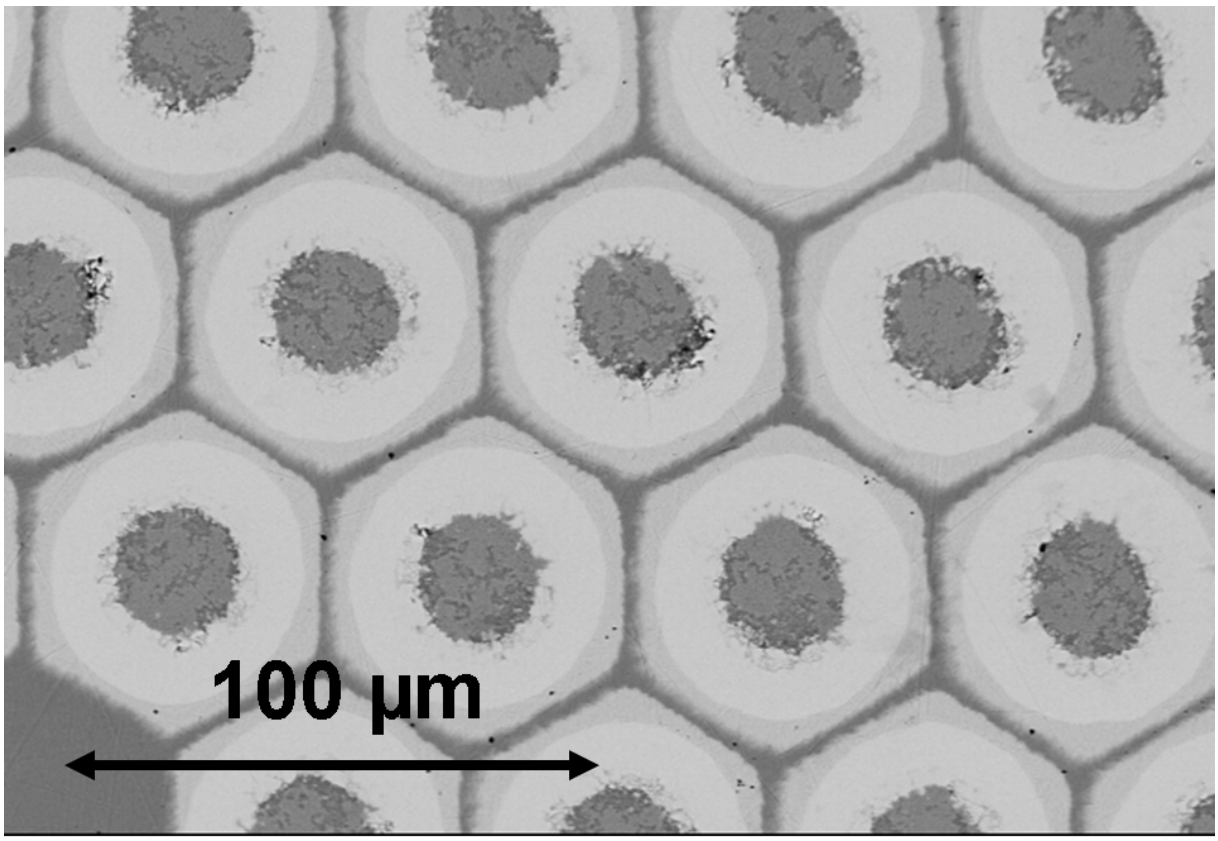

Figure. 1: Backscatter electron image of the PIT strand cross section after 84 h-675 °C HT. A phase contrast between reacted and non-reacted part of the tube can be seen. SEM image courtesy of G. Arnau, CERN TS-MME.

High resolution neutron diffraction measurements have been performed at the POLDI beamline of SINQ. In order to determine the transverse and axial lattice constants in the different strand phases, measurements were performed in two configurations with neutrons scattering at crystallographic planes either parallel or perpendicular to the strand axis (in the following referred to as transverse and axial directions, respectively). The instrument was calibrated using Si-powder from the National Institute of Standards and Technology (NIST, standard Reference Material 640c). All measurements were performed at room temperature (RT).

The Nb-Ta and $(Nb\text{-}Ta)_3Sn$ lattice constants have been measured using entire composite wires as well as reacted tubes that were extracted from the Cu matrix of the PIT strand by chemical etching. The Nb-Ta lattice parameter measured in the extracted tubes is about 3.301 Å (see Table 1), which corresponds with the lattice parameter measured at POLDI for annealed pure Nb. The $(Nb\text{-}Ta)_3Sn$ lattice constant determined using the extracted tubes is about 5.289 Å (Table 1). Differences in axial and transverse direction are smaller than the experimental error: in the extracted tubes $(Nb\text{-}Ta)_3Sn$ is in a nearly stress free state at RT.

Table 1: Axial and transverse $(Nb\text{-}Ta)_3Sn$ and Nb-Ta lattice parameters determined using tubes extracted from the Cu matrix of the reacted PIT strand.

	Lattice parameter (Å)
$(Nb\text{-}Ta)_3Sn$ (440) axial	5.28877±0.00056
$(Nb\text{-}Ta)_3Sn$ (321) transverse	5.28847±0.00062
Nb-Ta (110) axial	3.30055±0.00007
Nb-Ta (220) axial	3.30079±0.00012
Nb-Ta (211) transverse	3.30074±0.00018
Nb-Ta (110) transverse	3.30117±0.00019

The Sn content in the Nb_3Sn phase can vary between about 18-25 at.% Sn and the Nb_3Sn lattice parameter of stress relaxed Nb_3Sn increases linearly with increasing Sn content from about 5.28 to 5.29 Å.[10] The Sn content in the $(Nb\text{-}Ta)_3Sn$ filaments of the strand sample used here varies between 22-25 at.% (as determined by energy dispersive x-ray spectroscopy[11]), which is in agreement with the $(Nb\text{-}Ta)_3Sn$ lattice constant measured at POLDI.

For the determination of preferential crystalline orientation in the different strand phases, ten parallel aligned samples were turned from -90° to 20° with respect to the scattering vector. At 0° the scattering vector is in the direction of the strand axis. Diffraction measurements were done in 10° steps. The relative variations of the Cu, Nb-Ta and $(Nb\text{-}Ta)_3Sn$ peak intensities as a function of sample angle are plotted in Figures 2-a and 2-b, respectively.

After the 675 °C HT Cu exhibits a duplex texture with <111> and <200> orientations parallel to the strand axis. As observed in drawn Cu/Nb composite wires, the <111> texture is developed during the cold drawing process and the <200> component appears during the subsequent 675 °C HT.[12] It can be seen in Figure 2-b that after the 675 °C HT the Nb-Ta has a strong <110> texture parallel to the strand axis. This texture is similar to the one observed in severely cold drawn bcc Nb.[8, 12] The 675°C HT did not modify the Nb-Ta texture; indeed, Nb recrystallises at a much higher temperature (between 800°C and 1000°C depending on the cold worked state). Concerning the reacted phase, the (440) peak maximum at 0° shows that the $(Nb\text{-}Ta)_3Sn$ grains have also a preferential <110> orientation parallel to the strand axis. This texture is related to the initial texture of the Nb-Ta precursor filaments.[13]

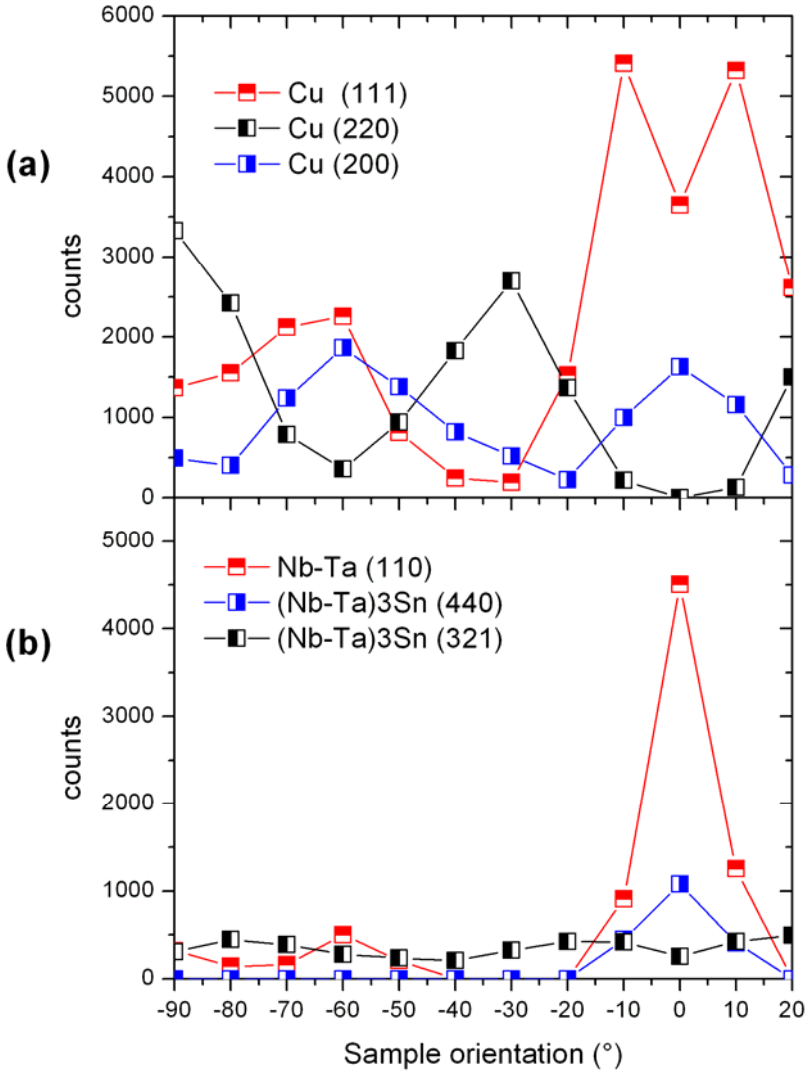

Figure 2: Diffraction peak intensity of selected peaks in (a) Cu and in (b) Nb-Ta and $(Nb\text{-}Ta)_3Sn$ as a function of strand orientation with respect to the neutron beam in the reacted PIT strand. At 0° the scattering vector is in direction of the strand axis.

In order to demonstrate the influence of the 675 °C HT on the load carrying capability of the different PIT strand phases, Figure 3 shows the lattice parameter variations in Cu (fig. 3-a), Nb-Ta grains (fig. 3-b) before and after HT and in $(Nb\text{-}Ta)_3Sn$ grains (fig. 3-c) after HT as a function of the macroscopic tensile stress. The error bars in the Figure represent the statistical uncertainty only, however, all systematical errors of the lattice parameters are small compared to the statistical ones. Lattice parameters have been plotted instead of strain values in order to avoid additional errors caused by uncertainties of the stress free lattice parameters. In the as-drawn state, i.e. in the non-heat treated strand, and prior to tensile loading Cu is under pre-compression in the axial direction ($a_{Cu} < 3.6155$ Å, the latter value being measured at POLDI for annealed pure Cu) as observed to a higher extent in Cu/Nb nanofilamentary wires obtained with a severe plastic deformation process based on cold drawing.[14] The Cu residual axial compression arises from the plastic mismatch between Cu and Nb with high yield stress Nb filaments imposing elevated back stress on the low

yield stress Cu matrix. The plastic mismatch is also demonstrated by the evolution of the lattice constant in Cu and Nb-Ta grains upon tensile loading: while the Cu lattice constant deviates from linearity and tends to level-off above an applied stress of 300 MPa (in agreement with the yield stress of cold worked Cu), the Nb-Ta lattice constant starts to increase faster above the same stress. Such a behavior evidences load transfer above 300 MPa from the plastifying Cu matrix into the Nb-Ta tubes mainly remaining in the elastic regime.

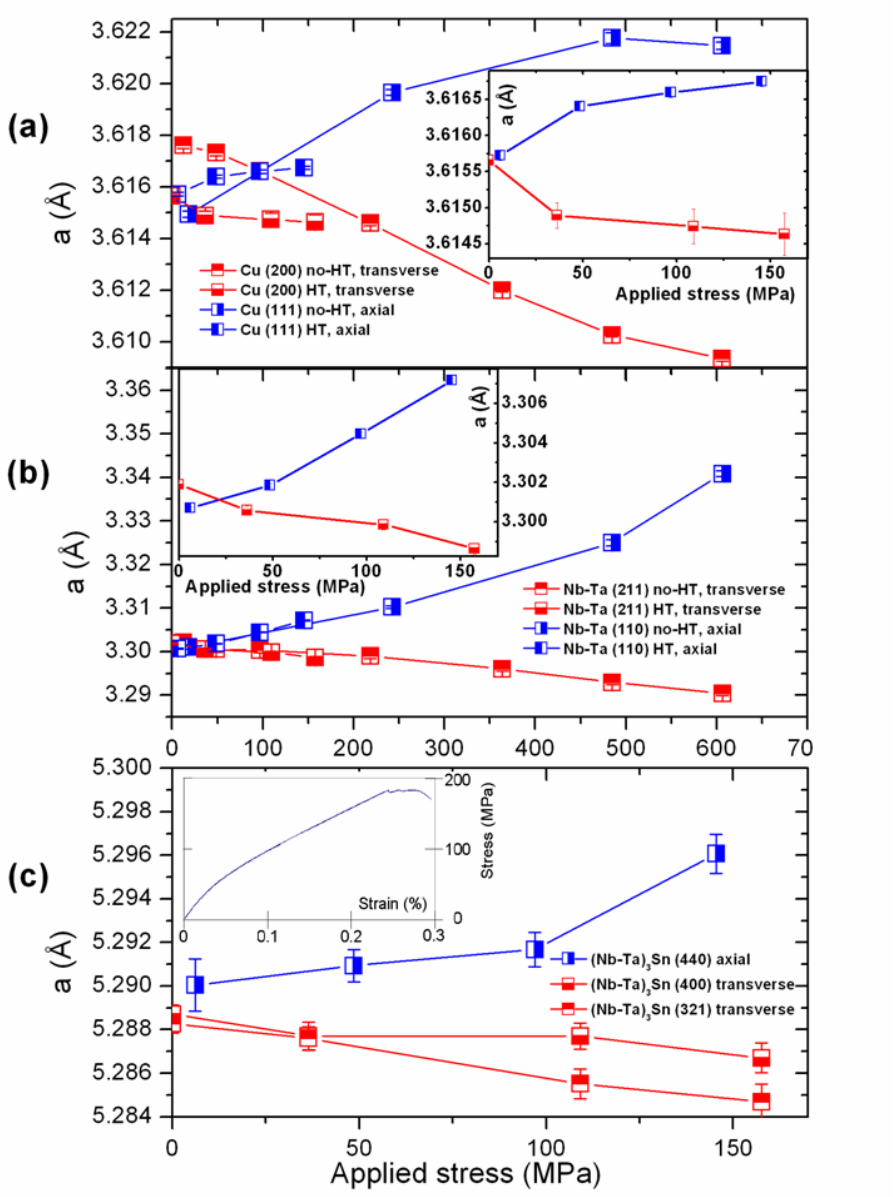

Figure 3: Cu, Nb-Ta and $(Nb\text{-}Ta)_3Sn$ elastic strain in axial and transverse direction as a function of uniaxial tensile stress. For Cu and Nb-Ta the elastic strain has been measured for the non-heat treated and 675 °C heat treated PIT strand. The Cu and Nb results for the reacted strand are magnified in insets (a) and (b). The error bars indicate a statistical error of ±1 σ. In axial wire position only the Nb_3Sn (440) reflection had sufficient intensity for determining the lattice spacing. In the inset in (c) the stress-strain curve obtained for the reacted PIT strand is shown (courtesy of B. Rehmer, BAM).

Differences of the stress free Cu, Nb-Ta and $(Nb\text{-}Ta)_3Sn$ lattice parameters and the lattice parameters of the corresponding phases in the reacted PIT strand in the absence of an external load are smaller than the experimental error. At RT $(Nb\text{-}Ta)_3Sn$ might be in slight residual axial tension. In the reacted wire the Cu matrix has lost almost entirely its load carrying ability with a yield stress below 50 MPa. As a consequence, in the reacted strand the tensile load is transferred onto the brittle $(Nb\text{-}Ta)_3Sn$ and the remaining Nb-Ta alloy, as indicated by the increase of the slope with which the Nb-Ta and $(Nb\text{-}Ta)_3Sn$ lattice constants increase in the axial direction above 100 MPa. At RT the PIT strand, which contains about 42 vol.% Cu, ruptures at a stress below 200 MPa and at a very low strain of about 0.3 % (see inset of figure 3-c).

In summary, the A15 phase formed during the 675 °C reaction HT exhibits a preferential <110> grain orientation parallel to the strand drawing axis. The anisotropic $(Nb\text{-}Ta)_3Sn$ grain orientation is a consequence of the texture of the Nb-Ta precursor that develops during the cold drawing process of the PIT strand prior to the reaction HT.

While the <110> texture may have only a small influence on the critical properties of the un-strained $(Nb\text{-}Ta)_3Sn$ [15], it might have a significant influence on the strain induced J_c degradation. It has to be noted that an external tensile load applied to the <110> oriented $(Nb\text{-}Ta)_3Sn$ grains causes an orthorhombic distortion of the lattice. The degree of $(Nb\text{-}Ta)_3Sn$ texture could possibly partly explain a J_c strain sensitivity dependence with respect to the process route.

In addition, no strong residual stresses have been measured at RT in the Nb-based phases of the reacted PIT strand, despite the mismatch of thermal expansion coefficients that could cause stresses upon cooling down from the reaction temperature to RT. This may be explained by the fact that the Cu matrix in the heat treated strand is so soft that the strain induced by different thermal contraction will cause mainly a plastic deformation of Cu so that residual stresses do not build up in Nb-Ta and $(Nb\text{-}Ta)_3Sn$. Finally, the results presented show that after the 675 °C HT the Cu matrix looses almost entirely its load carrying capability and any externally applied stress is mainly transferred to the remaining Nb-Ta alloy and to the brittle $(Nb\text{-}Ta)_3Sn$. This co-deformation mechanism needs to be considered when assessing the influence of the strand design on the strain induced degradation of Nb_3Sn superconductors.

We would like to thank R. Flükiger, B. Seeber and F. Buta of the Group of Applied Physics (GAP) of the University of Geneva and A. Godeke of the Lawrence Berkeley National Laboratory for fruitful discussions and suggestions. We acknowledge the PSI for neutron beam time at the POLDI experiment.

References

[1] B. Seeber, D. Uglietti, V. Abächerli, P.-A. Bovier, D. Eckert, G. Kübler, P. Lezza, A. Pollini, R. Flükiger, Review of Scientific Instruments 76, 093901, (2005)

[2] W. Goldacker, R. Flükiger, Journal de Physique 45, (1984), 387-390

[3] R. Flükiger, D. Uglietti, V. Abächerli, B. Seeber, Supercond. Sci. Technol. 18 (2005), 416-423

[4] W. Goldacker, R. Flükiger, IEEE Transactions on Magnetics, MAG-21(2), (1985), 807-810

[5] S. Awaji, H. Oguro, G. Nishijima, P. Badica, K. Watanabe, S. Harjo, T. Kamiyama, K. Katagiri, IEEE Trans. Appl. Supercon. 16(2), (2006), 1228-1231

[6] U. Stuhr, Nuclear Instruments and Methods in Physics research A 545, (2005), 319-329

[7] U. Stuhr, H. Spitzer, J. Egger, A. Hofer, P. Rasmussen, D. Graf, A. Bollhalder, M. Schild, G. Bauer, W. Wagner, Nuclear Instruments and Methods in Physics research A 545, (2005), 330-338

[8] L. Thilly, P.O. Renault, V. Vidal, F. Lecouturier, S. Van Petegem, U. Stuhr, H. Van Swygenhoven, A Appl. Phys. Lett. 88, 91906, (2006)

[9] J.L.H. Lindenhovius, E.M. Hornsveld, A. den Ouden, W.A.J. Wessel, H.H.J. ten Kate, IEEE Trans. Appl. Supercon., 10(1), (2000), 975-978

[10] H. Devantay, J.L. Jorda, M. Decroux, J. Müller, J. Mat. Sci. 16, (1981), 2145-2153

[11] P.-Y. Pfirter, M. Cantoni (dir), MSc thesis, EPFL Lausanne, (2006)

[12] V. Vidal, L. Thilly, F. Lecouturier, P.O. Renault, Scripta Materialia, 57-3 (2007), 245

[13] K. Togano, K. Tachikawa, J. Appl. Phys. 50(5), (1979), 3495-3499

[14] L. Thilly, S. Van Petegem, P.O. Renault, V. Vidal, F. Lecouturier, S. Brandstetter, B. Schmitt, H. Van Swygenhoven, Appl. Phys. Lett. 90, 241907, (2007)

[15] S. Foner, E.J. McNiff Jr, Phs. Lett. 58A, (1976), 318-320

[16] J.W. Ekin, N. Cheggour, M. Abrecht, C. Clickner, M. Field, S. Hong, J. Parrell, Y. Zhang, IEEE Trans. Appl. Supercon. 15(2), (2005), 3560-3563